

Title	Study of the kinetics and mechanism of rapid self-assembly in block copolymer thin films during solvo-microwave annealing
Authors	Mokarian-Tabari, Parvaneh; Cummins, Cian; Rasappa, Sozaraj; Simao, Claudia; Sotomayor Torres, Clivia M.; Holmes, Justin D.; Morris, Michael A.
Publication date	2014-08-19
Original Citation	MOKARIAN-TABARI, P., CUMMINS, C., RASAPPA, S., SIMAO, C., SOTOMAYOR TORRES, C. M., HOLMES, J. D. & MORRIS, M. A. 2014. Study of the Kinetics and Mechanism of Rapid Self-Assembly in Block Copolymer Thin Films during Solvo-Microwave Annealing. <i>Langmuir</i> , 30, 10728-10739. <a href="http://dx.doi.org/10.1021/la503137q">http://dx.doi.org/10.1021/la503137q</a>
Type of publication	Article (peer-reviewed)
Link to publisher's version	<a href="http://pubs.acs.org/doi/abs/10.1021/la503137q">http://pubs.acs.org/doi/abs/10.1021/la503137q</a> - <a href="http://dx.doi.org/10.1021/la503137q">10.1021/la503137q</a>
Rights	© 2014 American Chemical Society. This document is the Submitted Manuscript version of a Published Work that appeared in final form in <i>Langmuir</i> , copyright © American Chemical Society after peer review and technical editing by the publisher. To access the final edited and published work see <a href="http://pubs.acs.org/doi/pdf/10.1021/la503137q">http://pubs.acs.org/doi/pdf/10.1021/la503137q</a>
Download date	2024-05-29 18:41:42
Item downloaded from	<a href="https://hdl.handle.net/10468/2281">https://hdl.handle.net/10468/2281</a>



# UCC

**University College Cork, Ireland**  
Coláiste na hOllscoile Corcaigh

# A Study of the Kinetics and Mechanism of Rapid Self- assembly in Block Copolymer Thin Films during “Solvo-microwave” Annealing

*Parvaneh Mokarian-Tabari,<sup>1,2,\*</sup> Cian Cummins,<sup>1</sup> Sozaraj Rasappa,<sup>1,2,†</sup> Justin D. Holmes<sup>1,2</sup> and  
Michael A. Morris<sup>1,2</sup>*

(1) Department of Chemistry, University College Cork and Tyndall National Institute, Cork,  
Ireland.

(2) Centre for Research on Adaptive Nanostructures and Nanodevices (CRANN) and AMBER  
Centre, Trinity College Dublin, Dublin, Ireland.

\*Address correspondence to p.mokarian@ucc.ie

**ABSTRACT** Microwave annealing is an emerging technique for achieving ordered patterns of block copolymer films in substrates. Little is understood about the mechanisms of microphase separation during the microwave annealing process and how it promotes the micro phase separation of the blocks. Here, we use controlled power microwave irradiation in the presence of tetrahydrofuran (THF) solvent, to achieve lateral microphase separation in high- $\chi$  lamellar forming poly(styrene-*b*-lactic acid) PS-*b*-PLA. A highly ordered line pattern was formed within

seconds on a silicon substrate. *In-situ* temperature measurement of the silicon substrate coupled to condition changes during “solvo-microwave” annealing allowed understanding of the processes to be attained. Our results suggest that the substrate has little effect on the ordering process and is essentially microwave transparent but rather, it is direct heating of the polar THF molecules that causes microphase separation. It is postulated that the rapid interaction of THF with microwaves and the resultant temperature increase to 55 °C within seconds causes an increase of the vapor pressure of the solvent from 19.8 kPa to 70 kPa. This enriched vapor environment increases the plasticity of both PS and PLA chains and leads to the fast self-assembly kinetics. Comparing the patterns formed on silicon, germanium and silicon on insulator (SOI) and also an *in-situ* temperature measurement of silicon in the oven confirms the significance of the solvent over the role of substrate heating during “solvo-microwave” annealing. Besides the short annealing time which has technological importance, the coherence length is on a micron scale and dewetting is not observed after annealing. The etched pattern (PLA was removed by an Ar/O<sub>2</sub> reactive ion etch) was transferred to the underlying silicon substrate fabricating sub-20 nm Si nanowires over large areas demonstrating that the morphology is consistent both across and through the film.

**KEYWORDS:** Lamellar block copolymer self-assembly, Poly(styrene-*b*-lactic acid), microwave annealing, solvo-microwave annealing, Reactive Ion Etching (RIE), High- $\chi$  block copolymers, *in-situ* measurement

Self-assembled block copolymer (BCP) thin films are a potential candidate for fabrication of nanofeatures such as nanopillars, nanowires and nanowells beyond the capacity of current photolithography techniques. However long annealing times,<sup>1</sup> the lack of a defect free long range

order pattern, complex lift off and etch process<sup>2,3</sup> are some of the obstacles that need to be addressed for successful implementation of this technique for advanced patterning. Some of these issues can be improved by using a more strongly segregated or “high- $\chi$ ” block copolymer since as  $\chi$  increases one can move to lower molecular weights whilst maintaining the thermodynamic driving force for low defectivity, small feature size and increasing chemical contrast for improved etching or selected material inclusion.

Annealing times (since these systems do not usually spontaneously long-range order at room temperature) are critical as pattern quality is determined by the ability of a BCP to eliminate defects such as dislocations by chain motion.<sup>4</sup> Whilst in general morphological improvement is provided by higher  $\chi$  BCPs, it also reduces the kinetics of polymer diffusion during thermal annealing.<sup>4b</sup> With regard to thin films, molecules are restricted in their motions due to confinement effects. In lamellar forming block copolymers, the layered structure imposes additional constraints on the mobility and diffusion of the chains<sup>5</sup> which is an important factor for defect annihilation. The diffusion in perpendicular lamellar BCPs can happen along the domains (parallel diffusion), but the elimination of defects requires “hopping diffusion” which requires a chain to diffuse perpendicular to the interface.<sup>4b</sup> This involves a chain breaking away from the interface and relocating at opposite interface. The diffusion across a domain involves mixing within the domain. For high- $\chi$  BCPs, the increased penalty of mixing results in slower diffusion rate and higher kinetic barriers and subsequently leads to significantly longer annealing times.<sup>4-6</sup>

Microwave assisted microphase separation appears to offer considerable advantages in reducing annealing times in a number of BCP systems and we show that we can overcome long annealing times associated with a relatively high- $\chi$  poly(styrene-*b*-lactic acid) (PS-*b*-PLA) ( $\chi=0.19$ ) system by utilizing microwave energy. Microwave annealing was first demonstrated by

Zhang and Buriak.<sup>7,8</sup> So far, it has been employed for annealing commonly used poly(styrene-*b*-methyl methacrylate) (PS-*b*-PMMA)<sup>7,9,10</sup> and poly(styrene)-*b*-poly(2-vinylpyridine) (PS-*b*-P2VP)<sup>8,7,10</sup> block copolymers. Recently, the use of microwave has been demonstrated with poly(styrene-*b*-dimethylsiloxane) (PS-*b*-PDMS) system.<sup>9</sup> However, despite the promise of this technique, little is known about the mechanism of how microwave irradiation might sponsor the molecular motion that accompanies microphase separation. Buriak and coworkers have championed substrate heating as the primary source of molecular motion driven by defects in silicon substrates that absorb microwave radiation.<sup>10</sup> However, recent results within our group seem to indicate this may not be the case in all systems and have suggested that microwave absorption by the solvent molecules might also make a significant contribution to the annealing process. We have modified the system to carefully monitor temperature and extended the substrate range to amplify our model and this is reported here.

The PS-*b*-PLA system is of particular interest. PLA is a biodegradable aliphatic polyester and can be chemically etched to provide an on-chip etch mask for pattern transfer.<sup>11,12, 13</sup> In hexagonal forming PS-*b*-PLA the thermal annealing process can be very long (12 hours) and problematic due to thermal degradation of PLA.<sup>12,14</sup> Solvent annealing has been recently shown for PS-*b*-PLA seems more practical.<sup>11,15</sup> Recent reports have examined lamellar forming PS-*b*-PLA systems.<sup>16,17,18</sup> Depending on the difference in the surface energy of the substrate/air with each block or the confinement effect, the lamellae can align either perpendicular or parallel to the substrate.<sup>19</sup> To achieve perpendicular alignment, usually a surface modification step is required which is usually done by applying a SAM (self-assembled monolayer), a brush layer or chemical patterning of the substrate.<sup>20,21</sup> Surface modification is generally complicated and requires prolonged treatment periods. Previously, we have reported the perpendicular alignment of

lamellar PS-*b*-PEO systems through a stepwise thermo/solvent annealing system without any surface modification.<sup>22,23</sup> Here, we describe a simple and yet very fast technique for perpendicular alignment of the domains in lamellar PS-*b*-PLA diblock copolymer using a microwave unit in the presence of appropriate solvents which leads to formation of highly ordered patterns within 45 seconds. To understand the interaction of polymers with microwave irradiation, we carried out an *in-situ* temperature measurement of the substrate during the annealing. This provided a further insight on the microwave related process. This was followed by a reactive ion etch (RIE) step to remove PLA. We have measured the etch selectivity of PS and PLA in a controlled way by manipulating the DC bias indirectly. The remaining template was pattern transferred to the silicon substrate using an RIE-ICP (inductively coupled plasma) etcher, which led to fabrication of well-ordered 16 nm Si nanowires.

## **RESULTS AND DISCUSSIONS**

**The effect of temperature and time on “solvo-microwave” annealing.** Microwave annealing is a new recognized way of heating selected substrates rapidly and affecting phase separation in a short period of time.<sup>8</sup> Here we outline a new dynamic effect where substrates remain ‘cool’ and phase separation is brought about through “activation” of polar solvent molecules as discussed in details below. It should be initially pointed out that controlling and measuring the temperature during short microwave annealing periods is challenging as the power is varied (as in this set-up) or pulsed to effectively vary the temperature. During the user defined temperature ramp the power and hence temperature can fluctuate considerably. This causes some irregularity in results and therefore care must be taken. Moreover, the IR probe measures the temperature at the bottom of the microwave vessel rather than the silicon substrate (see Figure 5b). We tried different temperatures from 40-60 °C in the presence of different solvents and without solvent. In the

absence of solvent and with microwave annealing only, no phase separation was attained at temperatures below 60 °C.

The 200 nm thick PS-*b*-PLA films were exposed to THF at different temperatures during “solvo-microwave” annealing. A nominal power of 300 W, a ramp time of 5 min (unless otherwise stated) and an irradiation time of 30-120s was used. Note that here the applied powers were much less than 300 W, for example they were around 30 W for an anneal temperature of about 55 °C. 50 °C was observed as minimum temperature needed to observed phase separation even in the presence of THF. This is consistent with the known glass temperature ( $T_g$ ) of PLA in our PS-*b*-PLA system (49 °C), suggesting solvent swelling significantly reduces  $T_g$  in crystalline phase. Increasing the temperature above the  $T_g$  of PLA and from 52 °C to 57 °C improves the order in PS-*b*-PLA thin film. The AFM topographic image in Figure 1 shows the results at annealing temperature 52 °C. A poorly ordered phase separated pattern is observed after 60 s (Figure 1a) and increasing the time does not improve the long range order noticeably (Figure 1b). Note, it was not possible to maintain stable temperatures at anneal periods shorter than 60 s for temperatures less than about 55 °C.

The annealing temperature has a greater influence on enhancing the coherence length of the pattern in comparison to the annealing time. As shown is Figure 2, annealing at 57 °C for 30 s (Figure 2c) induces a better ordering rearrangement than annealing at 52 °C for 75 s or 54 °C for 60s (Figure 2a and 2b). However, note that anneal temperatures of 58 °C lead to dewetting of the film. We believe that the saturation vapor pressure during annealing has a profound effect. The vapor pressure of THF can be calculated using Antoine equation 1 below. A, B and C are Antoine constant and for  $23 < T < 100$  °C,  $A=6.99$ ,  $B=1202.29$  and  $C=226.254$  (gives the vapor pressure in mmHg).<sup>24</sup> THF has a vapor pressure of 19.8 kPa at room temperature. Increasing the

temperature above 58 °C raises the vapor pressure to 78 kPa and at this higher pressure, cooling and removal of the sample from the vial leads to condensation and dewetting.

$$P = 10^{A - \frac{B}{c+T}} \quad \text{eq. 1}$$

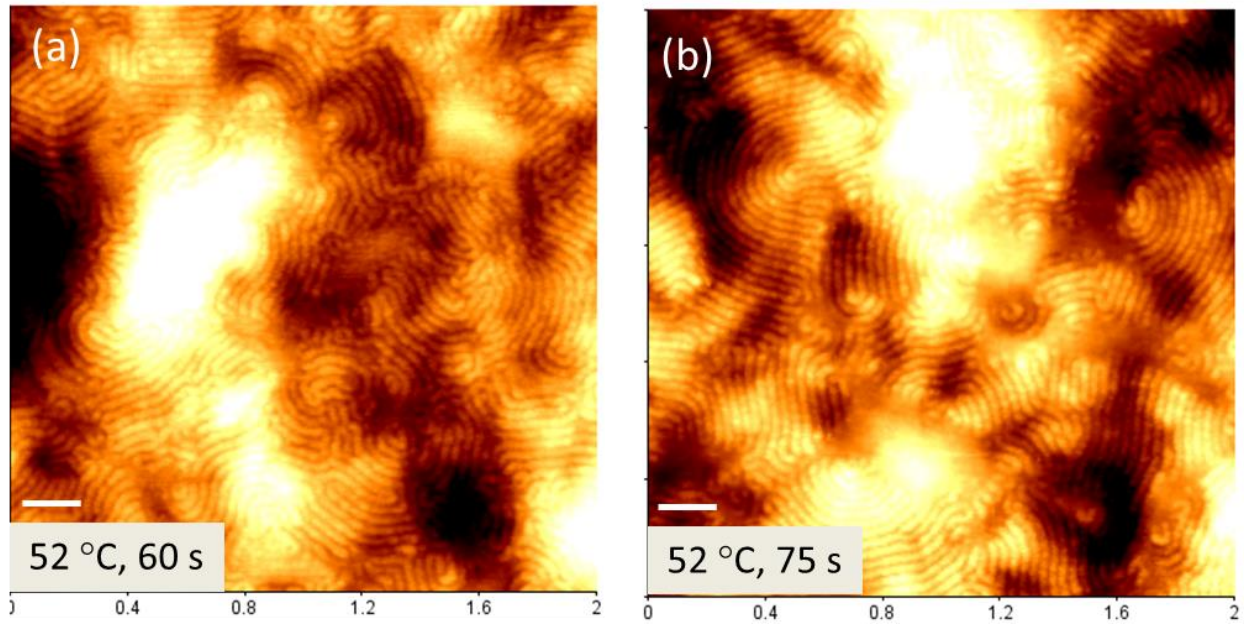


Figure 1. AFM topographic images showing poor phase separation of PS-*b*-PLA at 52 °C without surface modification. (a) After 60 s and (b) After 75 s. The scale bars are 200 nm.

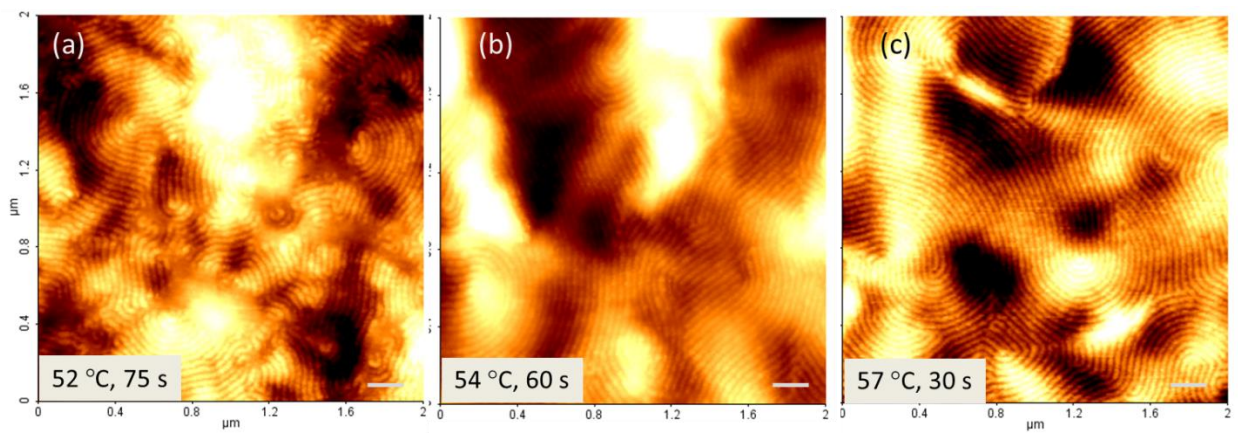




Figure 2. The higher impact of temperature over microwave annealing time on ordering of PS-*b*-PLA film. Higher temperature and lower annealing time (c) provides better degree of order than low temperature and longer annealing time (a) and (b). The scale bars are 200 nm.

**The choice of solvent for “solvo-microwave” annealing.** It was observed that the choice of solvent in “solvo-microwave” annealing follows similar rules to conventional solvent annealing, *i.e.* a neutral solvent for both blocks are required with added need for solvent molecule polarity in microwave annealing. We examined different annealing solvents including chloroform, acetone, toluene, tetrahydrofuran (THF), water and mixtures thereof. Table 1 shows the properties of the solvents and their affinity to PS and PLA. Apart from THF, none of the above mentioned solvents led to observable phase separation. Acetone is a polar solvent and PLA selective, while chloroform is non-polar and PS selective.<sup>11</sup> Annealing the PS-*b*-PLA either with acetone or chloroform did not induce lateral phase separation. The affinity of one block with the solvent, for example PLA with acetone will encourage migration of PLA to the surface to shield the PS chains from unfavorable contact with a non-solvent.<sup>11</sup> THF on the other hand is a polar solvent and selective for both PS and PLA. As there is no strong preference of the blocks to the solvent, the polymer/air surface will be neutral for both components. This provides an equal opportunity for either blocks to be present on the polymer/air interface and this will lead to lateral phase separation. The polar property of THF is the major advantage during microwave annealing. As a polar substance, THF can absorb microwave energy and heat up very fast which could subsequently lead to fast self-assembly route in PS-*b*-PLA film. This is discussed in more detail below in the *in-situ* temperature measurement experiment.

**Table 1.** The affinity of PS and PLA with different solvents.<sup>11, 25</sup>

<i>Solvent</i>	$\chi_{PS-Solvent}$	$\chi_{PLA-Solvent}$	<i>Selectivity</i>	<i>Polarity</i>
Acetone	1.30	0.28	PLA selective	Polar
Chloroform	0.34	<0.5	PS selective	Non-polar
Chlorobenzene	1.01	1.21	PS selective	Polar
THF	0.15	0.62	Neutral but slightly more selective for PS	Polar

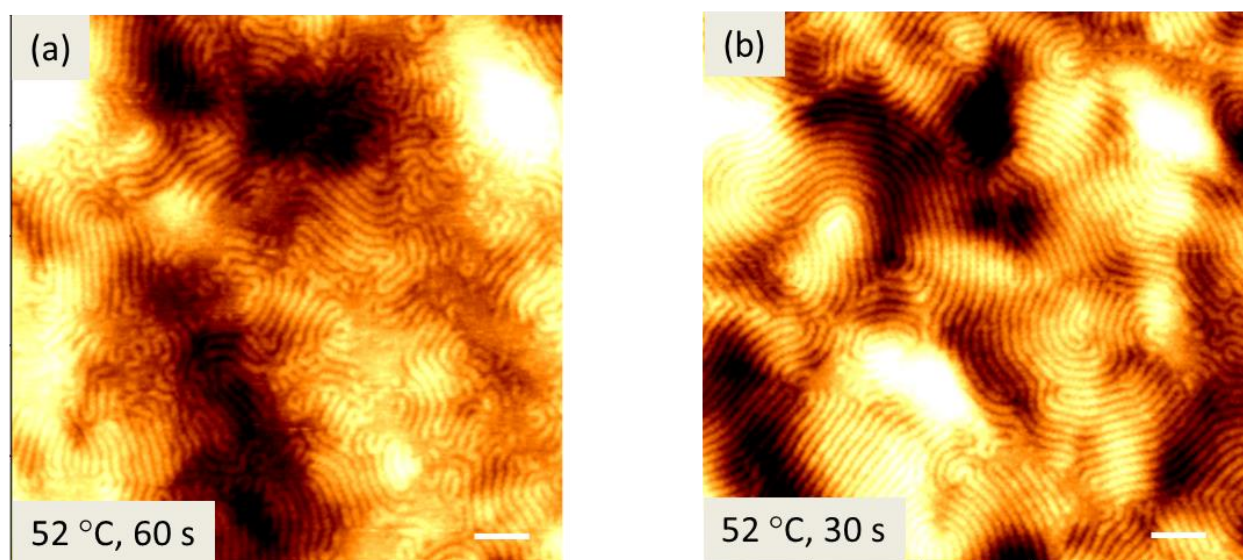


Figure 3. AFM topographic images showing the effect of cleaning the Si substrate prior to spin cast of PS-b-PLA film. (a) A poor phase separation without cleaning the substrate. (b) The improvement of long range order by sonicating the substrate in ethanol for 5 minutes. The scale bars are 200 nm.

The surface energy of PS and PLA are very close ( $\gamma^{PS} \sim 40.7 \text{ mJ/m}^2$  and  $\gamma^{PLA} \sim 38.3 \text{ mJ/m}^2$ ).<sup>26</sup> The neutrality of silicon surface for PS and PLA and also the neutrality of polymer/air surface

for both blocks when exposed to THF, provides an idea condition for perpendicular alignment of the domains on the Si substrate, provided that  $\chi N > 10.5$ . The Flory-Huggins interaction parameter ( $\chi$ ) between PS and PLA at a given temperature (T) can be calculated using equation 2 reported by Zalusky *et al.*:<sup>27</sup>

$$\chi(T) = \frac{98.1}{T} - 0.112 \quad \text{eq. 2}$$

The degree of polymerization for our PS-*b*-PLA system is calculated as  $N = 418.6$ . In our experimental conditions *i.e.*  $T \sim 55$  °C, the phase segregation strength  $\chi N$  is about 78 in upper limit of intermediate- segregation regime.<sup>28</sup> To improve the long range order and also the overall coverage of the samples, we cleaned the silicon substrate with ethanol and also exposed the sample to UV/Ozone for 45 minutes prior to casting. The samples were then microwaved annealed at 55 °C with THF. Figure 4 demonstrates the results following surface modification. A perpendicular alignment of lamellar domains was observed for both ethanol and UV/Ozone treated samples. However, the best patterns were achieved through UV/ozone treatment (Figure 4b). The pattern has a pitch of 34 nm. The PS domains were stained with  $\text{RuO}_4$  to increase the contrast for SEM imaging. Figure 4c is the cross section SEM image of the PS-*b*-PLA film after “solvo-microwave” annealing. The perpendicular domains of PS and PLA span the entire film thickness (200 nm) suggesting that the morphology is consistent through the film.

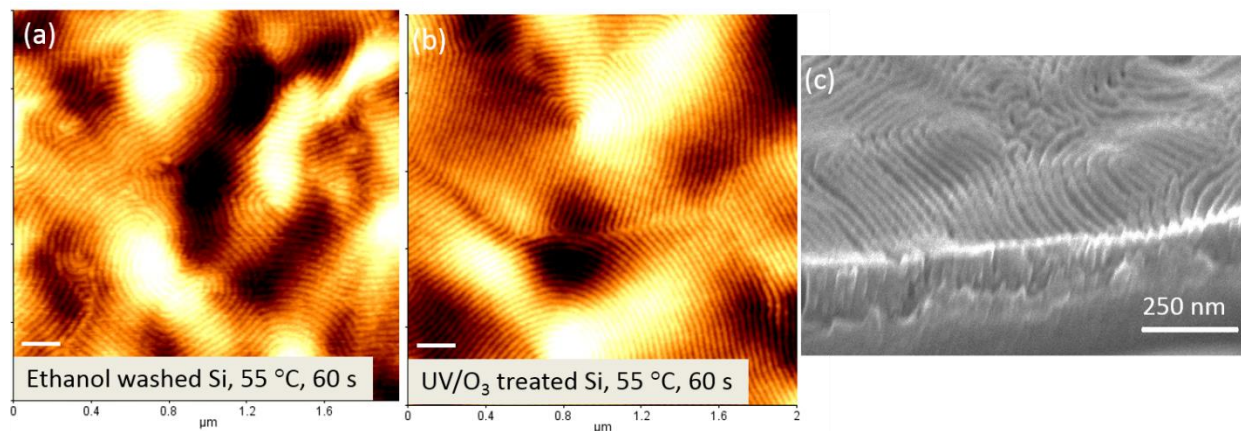


**Figure 4.** The effect UV/Ozone on long range order of PS-*b*-PLA thin film. The samples were “solvo-microwave” annealed at 55 °C for 60 s. The Si substrate was (a) Sonicated in ethanol for 10 minutes. (b) Exposed to UV/Ozone for 45 minutes. The UV/ozone surface treatment provides the best long range order. The pitch is 34 nm. The scale bars are 200 nm. (c) The SEM cross section shows the perpendicular domains span the entire film thickness.

***In-situ* temperature measurement of Si during microwave annealing.** Microwave is an electromagnetic wave that is absorbed by polar materials with electronegativity greater than 0.5.<sup>29</sup> When a polar material is exposed to microwave radiation, the molecules try to align themselves with respect to the alternating electromagnetic field. These oscillations are resisted by other intermolecular forces, and work done by the alternating electric field in overcoming these resistive forces manifest itself as heat.<sup>30,31,32</sup> There are three possibilities in microwave interaction with media; (1) purely thermal (kinetic), (2) microwave specific thermal and (3) microwave specific non-thermal interaction.<sup>30-31</sup> Silicon is transparent to electromagnetic radiation. However, impurity and dopants in silicon can lead to microwave absorption to some extent. Hung and Gliessman<sup>33</sup> were the first to observe impurity conduction in semiconductors. Soon after, the AC impurity conduction in Si was measured in the microwave frequency range.<sup>34</sup>

The concentration of impurity and whether an AC or DC current is applied can affect the microwave absorption in silicon. In order to understand the interaction of microwave with different components in our experiment (*i.e.*, substrates, polymers and solvents), we have carried out an *in-situ* temperature measurement of silicon by attaching an external temperature probe to the back of substrate and monitoring the temperature of silicon directly via the external sensor during exposure to microwave irradiation. Figure 5 shows the set up. More details can be found in experimental section. We used p-type silicon with a 2 nm native oxide layer on top. The purpose of the experiment was to investigate if there is an excessive heat rise in the silicon substrate during microwave irradiation which leads to fast-assembly of block copolymers. The result is shown in Figure 6. During microwave annealing in our experiment the temperature of the silicon substrate did not rise above the set value of 55 °C. Indeed, the temperature of the silicon substrate was ~20 °C less than the temperature of the glass vial (*i.e.* the control temperature of 55 °C). One assumes the dopant level in our silicon substrate is not high enough for significant microwave absorption either through ionized impurity pairs or due to the ‘hopping process’.<sup>35</sup> In the Zhang and Buriak *et al* work it has been shown that the resistivity of the substrate can affect the defect density in PS-*b*-P2VP film.<sup>7</sup> In Borah *et al* work<sup>9</sup> it was suggested that the substrate plays a passive role. In recently published work by Buriak *et al*,<sup>14</sup> it is shown that underlying silicon substrate is the key to the rapid heating observed. In our present study, it seems that the temperature rise through the heat transfer in the silicon substrate is not the major mechanism that results in the rapid self-assembly of PS-*b*-PLA films. It appears that that the high vapor pressure of THF and consequent increase in polymer swelling is at least partially responsible for the fast self-assembly of PS-*b*-PLA system. THF is a polar molecule that rapidly absorbs microwave radiation. As discussed above, the vapor pressure of THF at 55 °C is 3.5

times higher than at room temperature. We also cannot rule out the effect of having ‘hot’ THF molecules present in the film leading to heating and free volume inclusion. We will discuss it in more details in the next section.

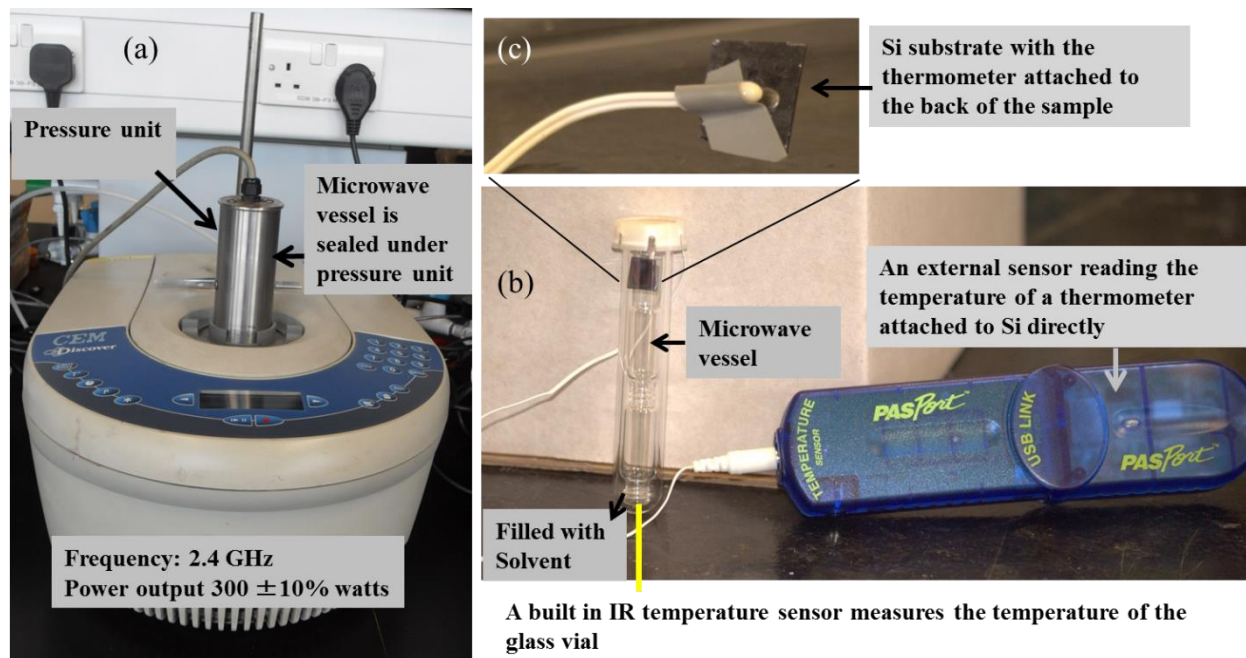


Figure 5. A 2.4 GHz Microwave unit. Pressure vessel (a) seals the microwave glass vessel shown in (b). The smaller glass vials in (b) are to hold the sample above the solvent level. A built in IR sensor measures the temperature at the bottom of the glass vial. (c) An external thermometer is attached to the silicon substrate and to a sensor (PASPort™). That sensor is linked to a laptop via a USB cable and reads the temperature of the silicon continuously during microwave annealing.

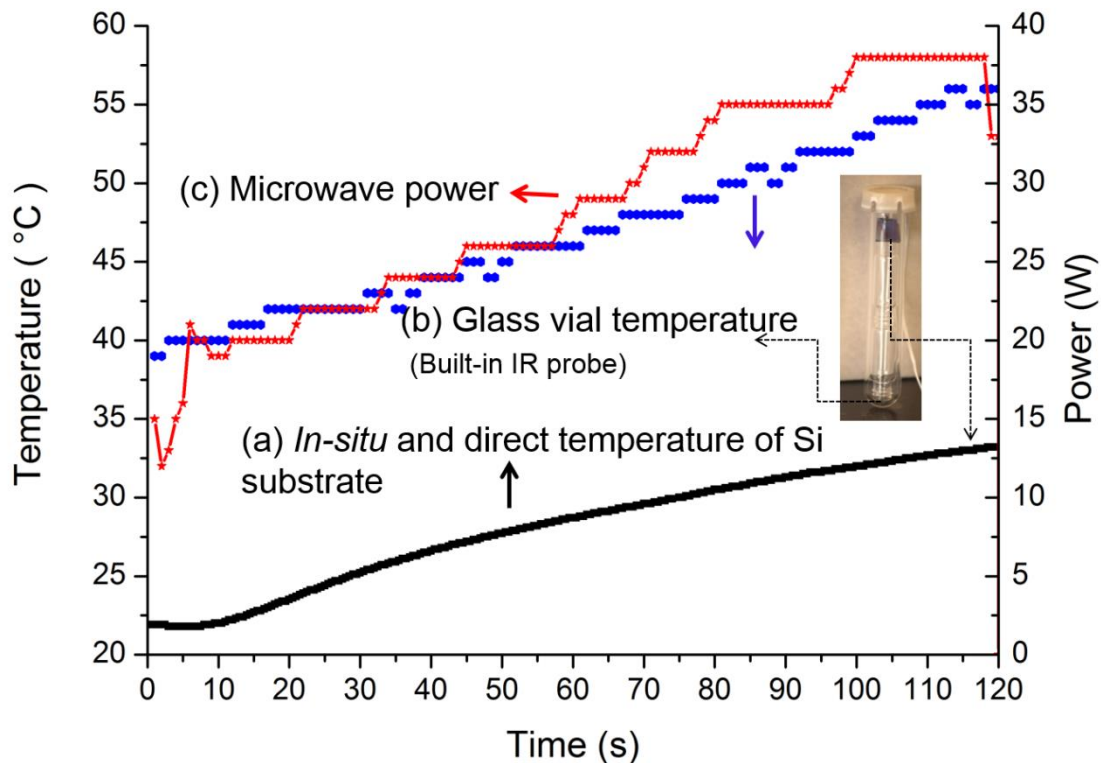


Figure 6. *In-situ* temperature measurement of silicon substrate during exposure to microwave radiation. (a) Direct temperature measurement of Si substrate by a thermometer attached at the back of the substrate and (b) the temperature of the glass vessel measured by a built-in IR probe during 120 s exposure and (c) microwave power range. The temperature of silicon substrate did not exceed the set value of 55 °C at any time during annealing.

**The mechanism of microwave assisted self-assembly.** To obtain a deeper insight into the underlying mechanism of self-assembly during microwave energy, we studied the PS-*b*-PLA films on different substrates *i.e.* silicon, germanium and silicon on insulator (SOI). In a recently published work by Buriak and co-workers<sup>10</sup> the heating of the substrate is considered the primary

source of heating and phase separation. However their observation is in absence of solvent and the temperature is much higher than our experimental condition ( $\sim 200$  °C). The effect of substrate during microwave irradiation can be studied from two different point of view; kinetics and thermodynamics. Our *in-situ* temperature measurement (Figure 6) showed that the temperature of silicon does not rise dramatically during solvo-microwave annealing and yet a rapid phase separation occurs within 60s. Although the possibility of direct microwave heating of the substrate seems to be a minor component of “solvo-microwave” annealing, it was considered worthwhile investigating the effect of the substrate on the kinetics of pattern formation during microwave annealing. Thus, we repeated the experiment on germanium substrate which has a higher dielectric constant ( $k=16$ ) than silicon ( $k=12$ ) and SOI (silicon on insulator with 140 nm buried oxide layer). If the substrate employed for microwave irradiation experiments is the primary basis to induce fast kinetics, it should take longer for PS-*b*-PLA film to phase separate on germanium than on silicon as it takes longer to heat up due to its higher dielectric constant. However, despite this assumption our result shows that in fact phase separation of PS-*b*-PLA film can happen almost twice as fast on germanium than on silicon and also at a slightly lower temperature (See Figure 7). These results emphasises the significant contributing influence of solvent vapor that acts as a plasticizer for rapid BCP self-assembly regardless of the substrate used. However, comparing the PS-*b*-PLA films on both silicon and germanium substrates (Figure 7a and b), one clearly observes that the coherence length is longer on silicon than on germanium. We expected to see a similar trend for an SOI substrate, but as shown in the topographic AFM image in Figure 7c, the annealing time on SOI substrate is noticeably longer than silicon and germanium substrate. For successful PS-*b*-PLA self-assembly on SOI, films required 3 minutes of microwave and solvent vapor annealing. This is perhaps due to the



existence of the buried oxide layer (140 nm thick) in the substrate that increases the resistivity of the substrate. However, these observations initially lead to contradicting assumption. The question arises; if the resistivity of the substrate has a significant role in kinetics of phase separation during solvo-microwave annealing (observed from comparing the results for Si with SOI), why does it take a shorter experimental treatment for self-assembly of the film on germanium which has a higher dielectric constant than silicon? To obtain more insight about the role of the substrate, we carried out an in-situ temperature measurement on PS-*b*-PLA film on silicon in the oven. The conditions were similar to the experiment in the microwave. The film was put inside an enclosed glass jar with a 2-5  $\mu\text{l}$  THF next to it at 55 °C. A thermometer was attached at the back of the substrate and the temperature of the silicon was monitored. As shown in the graph in Figure 8 the temperature of silicon rises immediately after putting the sample in the oven and it reaches 32 °C (similar to silicon temperature in the microwave) in less than 3 minutes. If the temperature of substrate was the main source of self-assembly, phase separation would be observed on the film annealed in the oven after keeping the sample at 32 °C for two minutes (a similar time to “solvo- microwave” annealing condition). However, no lateral phase separation was observed even after 10 minutes (see inset (a) in Figure 8). Evidently, this is linked to THF which has not reached the threshold vapor pressure of 70 kPa at 55 °C as described earlier. It takes 24 minutes for silicon to reach the set temperature of 55 °C. After reaching 55 °C, we kept the sample in the oven for 2 minutes (similar to microwave annealing condition) and then removed the sample, *i.e.*, after 26 minutes solvent annealing. As shown in inset (b) in Figure 8, a phase separated pattern forms. This is because the vapor pressure of THF has reached a minimum threshold to induce phase separation of the PS-*b*-PLA BCP. However, after one compares the phase separated pattern obtained with microwave annealing (Figure 4b) with

solvent annealing in the oven (Figure 8b), it is obvious that the former has a much better long range order. During “solvo-microwave” annealing, THF which is a polar solvent absorbs microwave energy once exposed to microwave irradiation. This leads to a rapid rise of the solvent vapor pressure in a very short time. Subsequent diffusion of the solvent vapor through the voids and free volume in the polymer network swells and mobilizes the polymer chains and contributes to fast self-assembly of the film. In the oven, on the other hand, THF heats up through a different mechanism. The heating in the oven is through convection and conduction and therefore it takes longer for THF to reach and built up the suitable pressure (nominal pressure: 70 kPa at 55 °C) to trigger a swift phase separation in PS-*b*-PLA film. In normal annealing in the oven, the solvent molecules have a thermal energy profile (*i.e.* vibration) however, in microwave they are electronically, rotationally excited and have high energy states besides thermal. During microwave annealing, some very high energy states can be created. These additional energies pass into the polymer causing efficient local heating.

The comparison of the “solvo-microwave” annealing process in the microwave and the oven confirms that in our case study PS-*b*-PLA system, the fast self- assembly is a kinetics effect majorly governed by solvent vapor pressure. However, the substrate plays a secondary role. There might be a threshold for the temperature of the substrate and this is the subject of future works. Nevertheless, the chemistry between the substrate and the polymers affects the degree of the order in the pattern and uniformity of the film shown in Figure 7.

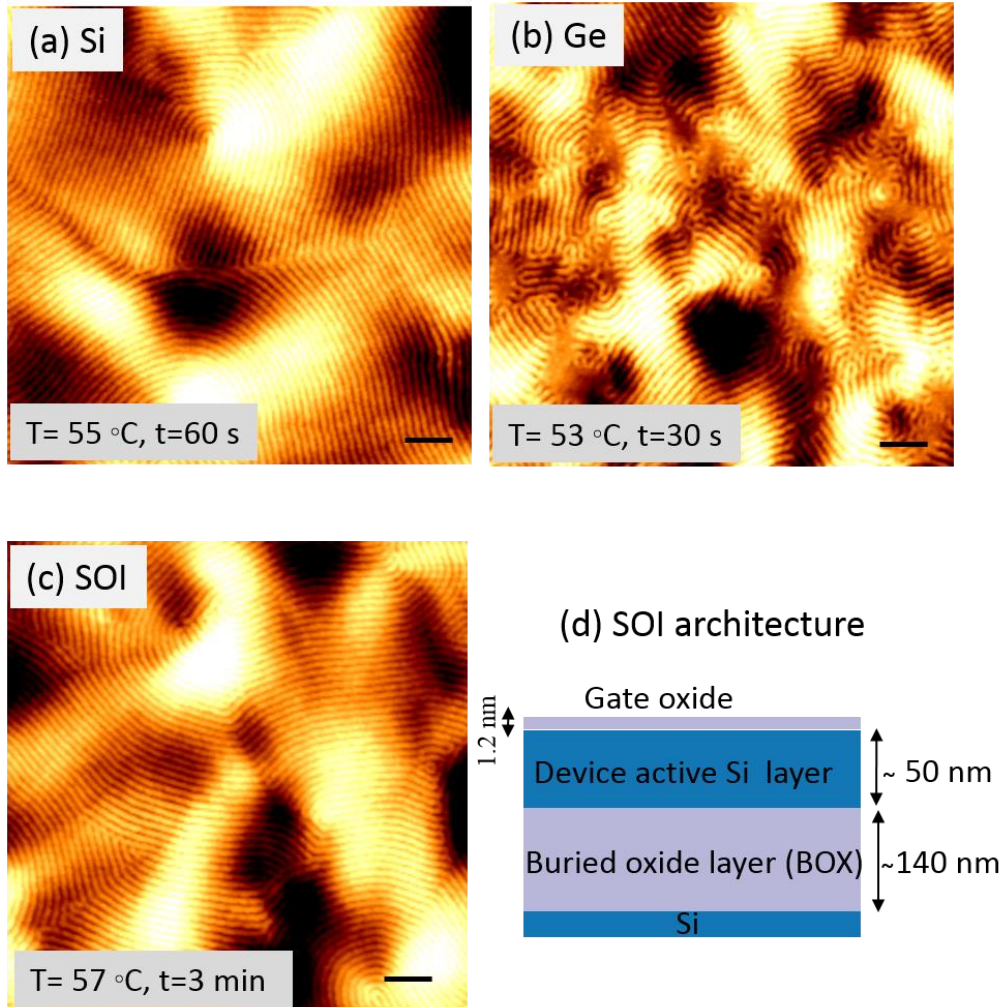


Figure 7. AFM topography images of “solvo-microwave” annealing of PS-*b*-PLA film on different substrates. (a) On Si, (b) on Ge and (c) on SOI substrate. (d) The schematic architecture of SOI in (c) with 140 nm buried oxide layer. The scale bars are 200 nm.

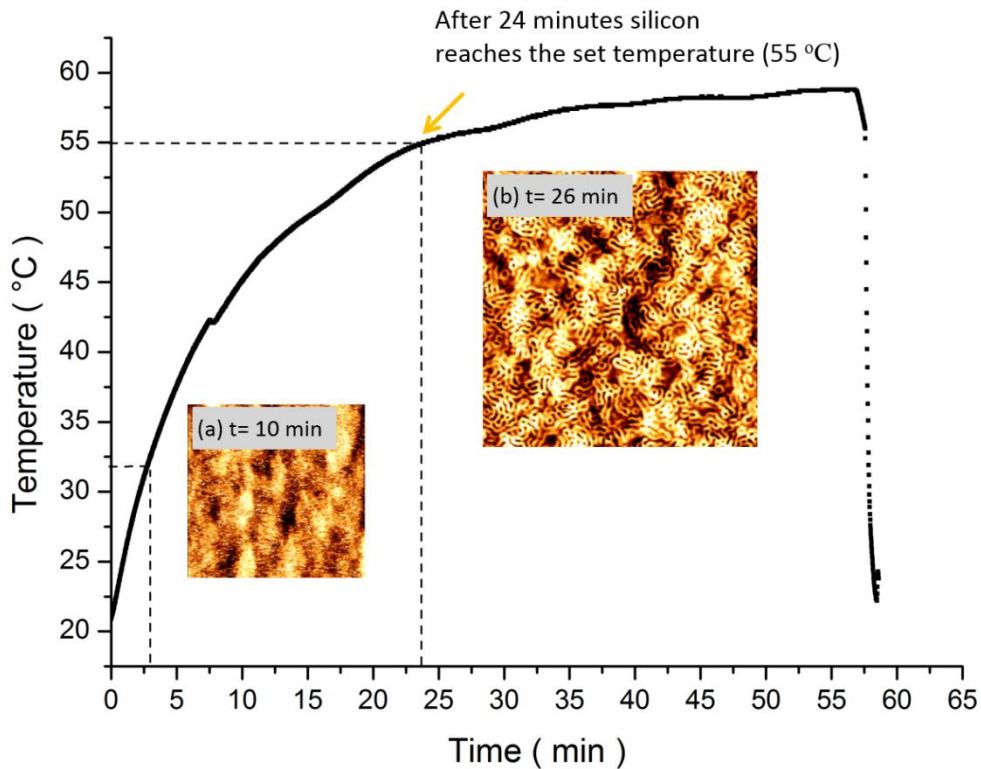


Figure 8. An *in-situ* temperature measurement of the silicon substrate during solvent annealing in the oven at 55 °C and with THF. The inset (a) is an AFM topography image of PS-*b*-PLA film after 10 minutes annealing which shows no phase separation and inset (b) is after 26 minutes (2 minutes after Si reached 55 °C). Both AFM topography images are 2x2 micron.

**Etch and pattern transfer.** In order to show that the pattern morphology exists throughout the depth of the film and the technique could be applied for generation of silicon circuit elements, a successful recipe was developed for partial removal of PLA using a dry etch procedure performed in an Oxford Instruments Plasmatech in RIE mode using a mixture of Ar/O<sub>2</sub> gas. We also tried different wet etch processes. The comparison of the methods and a detailed etch study of PS-*b*-PLA is published separately<sup>36</sup> and will not be presented here. It has been shown that the etch rate of polymers is related to sputtering factor.<sup>37</sup> Since carbon has a small sputtering yield,

therefore the etching of the carbon will be the slowest and hence the rate determining step. The etch rate is inversely proportional to the number of carbon atoms. On the other hand the number of oxygen atoms in a monomer enhance the etch rate according to the Ohnishi parameter determined from equation 3: <sup>37</sup>

$$v \propto \frac{N}{N_C - N_O} \quad \text{eq.3}$$

Whereas  $v$  is the etch rate,  $N$  is the total number of atoms in a monomer unit,  $N_C$  and  $N_O$  are the number of carbon and oxygen atoms in a monomer unit. Using equation 3, the etch rate of PS ( $C_8H_8$ ) and PLA ( $C_3H_6O_3$ ) can be calculated. However, as the number of carbon and oxygen in PLA are the same, the etch rate of PLA cannot be calculated theoretically. We determined the etch rate of PS and PLA experimentally. The etch rate of PS and PLA homopolymer is compared in Figure 10. Although the etch rate of PS is higher at the beginning, PLA etch rate increases at a later stage ( $t > 20$  s). Comparing the insets (topographic AFM images) in Figure 10, it seems that the etch is not one dimensional and removes the polymer laterally as well. The higher etch rate of PLA is correlated to higher number of oxygen atoms in the monomer. However, PLA contains C=O groups in its chain. C=O groups have much higher sputtering yield than carbon (there is no oxygen atom in PS chain). The C=O group in PLA is responsible for initial slower etch rate compared to PS. However, at longer etch times when C=O bond is broken, PLA etch rate accelerates.

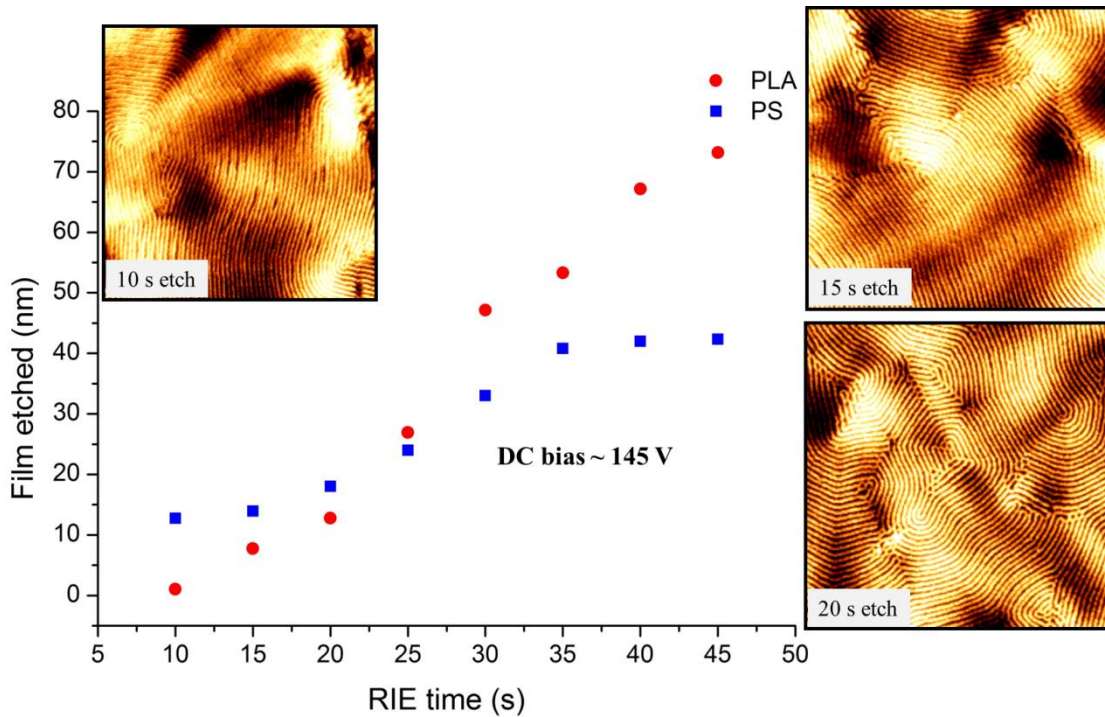


Figure 10. The etch rate of PS and PLA homopolymers in RIE at DC bias 145 V. Initially PLA shows slower etch rate due to high sputtering yield C=O group, but after 20 seconds when the C=O bond is broken, PLA is etched faster than PS. The insets are the topographic AFM images of PS-*b*-PLA after 10, 15 and 20 s etch time.

Figure 11 shows the top down and SEM cross section image of the film after the etch and pattern transfer. The remaining PS mask after the PLA etch was pattern transferred to a silicon substrate using a SF<sub>6</sub>/ C<sub>4</sub>F<sub>8</sub> etch<sup>3</sup> followed by a thermal oxidation step to remove all traces of polymer. The silicon nanowires shown in Figure 10 are 16 nm wide and 45 nm high.

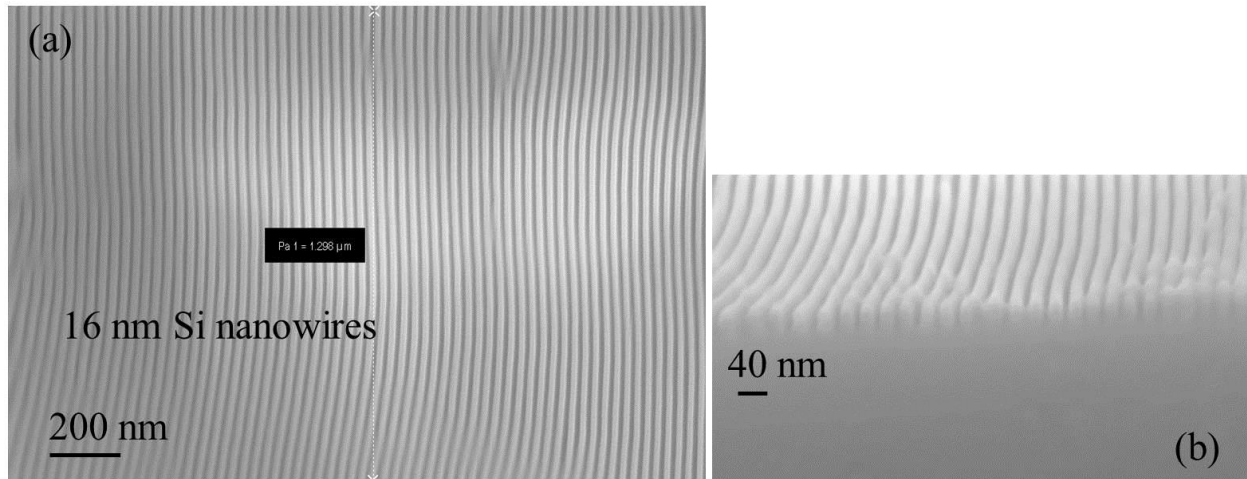


Figure 11. 16 nm Si nanowires fabricated by using PS-*b*-PLA as a template after 60 s “solvo-microwave” annealing with THF and 25 s RIE etch, followed by RIE- ICP pattern transfer. (a) Top-down SEM image and (b) SEM cross section of sample (a).

## CONCLUSIONS

We have demonstrated fast self-assembly of a high- $\chi$ , lamellar PS-*b*-PLA thin film utilizing microwave irradiation in presence of THF for 60 seconds. UV/ozone treatment of silicon substrate prior to spin cast improves the long range order dramatically. To probe the route of fast self-assembly of PS-*b*-PLA during ‘solvo-microwave’ annealing, we carried out an *in-situ* temperature measurement of silicon by attaching an external thermometer at the back of the substrate and recording the temperature of silicon. Our results show the temperature of silicon does not rise excessively during “solvo-microwave” annealing. Considering Si and SiO<sub>2</sub> are not polar, they do not absorb microwave energy. Therefore the heat transfer happens through conduction and convection rather than microwave absorption. With the range of temperature we applied (less than 60 °C), although the temperature in silicon rises rapidly, it is not high enough (~32 °C) to lead to fast self-assembly in such a short period of time. We suggest that polar THF

that absorbs electromagnetic radiation in microwave range plays a major role in rapid self-assembly process observed. The nominal vapor pressure of THF increases from 19.8 kPa at room temperature to 70 kPa at 55 °C within seconds of microwave exposure. The high vapor pressure of THF in a sealed vessel provides a fast access for diffusion to the depth of the film which gives the chains enough mobility to phase separate into well ordered domains. Comparing the *in-situ* temperature measurement of silicon in the microwave and in the oven confirms our theory that the substrate has a less important role during “solvo-microwave” annealing in comparison to the use of solvent. In the oven, silicon reached the temperature of 32 °C in less than 3 minutes and no phase separation was observed, whereas during the “solvo-microwave” annealing while the silicon reaches the same temperature, a long range order pattern forms. The reason is in the oven at 32 °C, the vapor pressure of THF is not high enough to make the film swell sufficiently at that period of time. During ‘solvo-microwave’ annealing, on the other hand, some very high energy states can be created as polar THF absorbs microwave energy very fast. These additional energies can pass into the polymer causing efficient local heating which leads to fast self-assembly effect.

Leaving the film in the oven for longer time, a phase separated pattern is observed, but it is poorer than the pattern obtained by microwave. This suggests that kinetics *i.e.* the rate of film swelling and diffusion affects the order and the coherence length of the pattern. Nevertheless, there might be a threshold for temperature of the substrate to initiate self-assembly. “Solvo-microwave” annealing of PS-*b*-PLA film on germanium substrate which has a higher dielectric constant than silicon but takes a shorter time than silicon, confirms the key role of THF as the primary cause of rapid self-assembly. On the other hand, longer annealing time was required for an SOI substrate that has a thicker buried oxide layer and thus higher dielectric constant than



silicon. The longer annealing time needed for SOI substrates suggests a possible minimum substrate temperature is required for effective pattern formation of block copolymers during “solvo-microwave” annealing. We measured the etch rate of PS and PLA homopolymers experimentally. PLA is etched faster due to the presence of oxygen in the back chain. Following an RIE-ICP etch a successful pattern transfer led to fabrication of 16 nm silicon nanowires. Our process provides a simple and effective means of pattern formation for an on-chip etch mask.

## EXPERIMENTAL

**Materials.** Lamellar forming (PS-*b*-PLA) block copolymer was purchased from Polymer Source with number average molecular weight of  $M_{n,PS} = 21 \text{ kg mol}^{-1}$  and  $M_{n,PLA} = 19.5 \text{ kg mol}^{-1}$ ,  $f_{PS}^v = 0.55$ , PDI:1.06. The block copolymer was used without any further modifications. Thin films of PS-*b*-PLA films were spun cast from 2 wt% chloroform solution on to silicon substrates. The properties of the PS-*b*-PLA are summarized in table 2.

Table 2. The properties of PS-*b*-PLA diblock copolymer based on the supplier’s data sheet.

Sample	$M_{n,PS}$ ( $\text{kg mol}^{-1}$ )	$M_{n,PLA}$ ( $\text{kg mol}^{-1}$ )	$f_{PS}^v$	$T_{PS}^g$ ( $^{\circ}\text{C}$ )	$T_{PLA}^g$ ( $^{\circ}\text{C}$ )
PS- <i>b</i> -PLA	19.5	24.5	0.55	98	49

$f_{PS}^v$ ,  $T_{PS}^g$ , and  $T_{PLA}^g$  are the volume fraction and glass transition of PS and PLA.

**Substrate preparation.** The Si substrates were sonicated in different solvents such as ethanol, acetone and isopropanol. However, they all result in poor phase separation under “solvo-

microwave” annealing. Best results were achieved when samples were exposed to UV/ozone for 45 minutes prior to spin casting.

**Solvo-microwave annealing and in-situ temperature measurement.** Figure 5 shows the industrial microwave unit we used to process the samples. In Figure 5b the microwave vial is displayed. The temperature is controlled at the bottom of the vial with an infrared (IR) probe. We used two smaller glass vials to raise the level of the solvent and also to provide a support base to hold the substrate. The power was set at 300 watts and a range of temperatures were tested. However, as the temperature range in our experiments was not too high (50-60 °C), in practice only small power (less than 50 watt) was applied to reach the set temperature. A range of thermal and solvent annealing steps in tetrahydrofuran, toluene, water, chloroform, acetone and mixtures thereof were tested up to 70 °C in the microwave.

**Etch and pattern transfer.** To measure the etch rate of PS and PLA, the homopolymers of PS and PLA with number average molecular weight of  $M_{n,PS} = 16 \text{ kg mol}^{-1}$ , PDI= 1.03 and  $M_{n,PLA} = 16 \text{ kg mol}^{-1}$ , PDI= 1.30 were etched at the same time with PS-*b*-PLA films. The dry etch was performed in an Oxford Instruments Plasmatech in RIE (reactive ion etching) mode using a mixture of argon: 15 sccm and O<sub>2</sub>: 10 sccm, at the process pressure of 12 mTorr and RF power of 40 W and DC bias 145 V. The remaining PS mask was pattern transferred to a silicon substrate using a combination of sulphur hexafluoride (SF<sub>6</sub>) and trifluoromethane (CHF<sub>3</sub>) gasses in an STS AOE inductively coupled plasma (ICP) etcher.<sup>3</sup> The residual PS stripes after the pattern transfer were removed by O<sub>2</sub> plasma.

**Film characterisation.** Atomic Force Microscopy (AFM) (Park systems, XE-100) was operated in AC (tapping) mode under ambient conditions using silicon micro cantilever probe tips with a force constant of 42 N m<sup>-1</sup>. Topographic and phase images were recorded simultaneously.

Scanning Electron Microscopy (SEM) images were obtained by a FEI Helios Nanolab 600i system at an accelerating voltage of 5 kV and at a working distance of 4 mm. Cross section SEM images involved cleaving the substrate in half and positioning the substrate perpendicular to the incident beam of electrons. The stage was then tilted at 20°. To achieve a contrast between PS and PLA in SEM and prior to etch, the PS domains were stained by ruthenium tetroxide.<sup>38</sup> A solution of ruthenium tetroxide was prepared by mixing ruthenium trichloride hydrate (Sigma) with active chlorine aqueous sodium hypochlorite (Sigma). 0.1 g of ruthenium trichloride hydrate was weighed out and in a fumehood 5 ml of 13 % active chlorine aqueous sodium hypochlorite was slowly added. This was then placed in a small desiccator with the cleaved film as seen in Figure 4c to selectively stain PS domains with RuO<sub>4</sub> vapors and provide contrast for SEM characterization. Note that caution should be taken when using RuO<sub>4</sub> and organic solvents should not come in to contact with the substance.

† Present address: Department of Micro and Nanotechnology, Technical University of Denmark, Denmark.

### **Author Contributions**

The manuscript was written through contributions of all authors. All authors have given approval to the final version of the manuscript.

### **Funding Sources**

We gratefully acknowledge Science Foundation Ireland (SFI) CSET/ CRANN and LAMAND NMP FP7 grant for funding this project.

Conflict of Interest: The authors declare no competing financial interest

## ACKNOWLEDGMENT

The authors thank Peter Gleeson and Matthew Shaw, staff of Intel and the AML (Advanced Microscopy Laboratory) in CRANN for assistance in microscopy.

## REFERENCES AND NOTES

1. Herr, D. J. C., Directed block copolymer self-assembly for nanoelectronics fabrication. *Journal of Materials Research* **2011**, *26* (2), 122-139
2. Farrell, R. A.; Petkov, N.; Shaw, M. T.; Djara, V.; Holmes, J. D.; Morris, M. A., Monitoring PMMA Elimination by Reactive Ion Etching from a Lamellar PS-b-PMMA Thin Film by ex Situ TEM Methods. *Macromolecules* **2010**, *43* (20), 8651-8655.
3. Borah, D.; Shaw, M. T.; Rasappa, S.; Farrell, R. A.; O'Mahony, C.; Faulkner, C. M.; Bosea, M.; Gleeson, P.; Holmes, J. D.; Morris, M. A., Plasma etch technologies for the development of ultra-small feature size transistor devices. *J. Phys. D-Appl. Phys.* **2011**, *44* (17), 12.
4. (a) Takahashi, H.; Laachi, N.; Delaney, K. T.; Hur, S. M.; Weinheimer, C. J.; Shykind, D.; Fredrickson, G. H., Defectivity in Laterally Confined Lamella-Forming Diblock Copolymers: Thermodynamic and Kinetic Aspects. *Macromolecules* **2012**, *45* (15), 6253-6265; (b) Chang, S.-W.; Vogel, E. E.; Ginzburg, V. V.; Murray, D. J.; Kramer, J. W.; Weinhold, J. D.; Chuang, V. P. W.; Sharma, R.; Evans, J. P.; Landes, B.; Ge, S.; Trefonas, P.; Hustad, P. D. In *Designing new materials and processes for directed self-assembly applications*, Proc. SPIE 8323, Alternative Lithographic Technologies IV, 2012; pp 83231M-83231M-9.
5. Lodge, T. P.; Dalvi, M. C., Mechanisms of Chain Diffusion in Lamellar Block-copolymers. *Physical Review Letters* **1995**, *75* (4), 657-660.
6. Yokoyama, H., Diffusion of block copolymers. *Materials Science & Engineering R-Reports* **2006**, *53* (5-6), 199-248.
7. Zhang, X. J.; Harns, K. D.; Wu, N. L. Y.; Murphy, J. N.; Buriak, J. M., Fast Assembly of Ordered Block Copolymer Nanostructures through Microwave Annealing. *ACS Nano* **2010**, *4* (11), 7021-7029.
8. Zhang, X. J.; Murphy, J. N.; Wu, N. L. Y.; Harris, K. D.; Buriak, J. M., Rapid Assembly of Nano lines with Precisely Controlled Spacing from Binary Blends of Block Copolymers. *Macromolecules* **2011**, *44* (24), 9752-9757.
9. Borah, D.; Sentharamaikannan, R.; Rasappa, S.; Kosmala, B.; Holmes, J. D.; Morris, M. A., Swift Nanopattern Formation of PS-b-PMMA and PS-b-PDMS Block Copolymer Films Using a Microwave Assisted Technique. *Acs Nano* **2013**, *7* (8), 6583-96.
10. Cong Jin, J. N. M., Kenneth D. Harris, Jillian M. Buriak,, Deconvoluting the Mechanism of Microwave Annealing of Block Copolymer Thin Films. *ACS Nano* **2014**, DOI: 10.1021/nn5009098.
11. Vayer, M.; Hillmyer, M. A.; Dirany, M.; Thevenin, G.; Erre, R.; Sinturel, C., Perpendicular orientation of cylindrical domains upon solvent annealing thin films of polystyrene-b-poly lactide. *Thin Solid Films* **2010**, *518* (14), 3710-3715.

12. Olayo-Valles, R.; Guo, S. W.; Lund, M. S.; Leighton, C.; Hillmyer, M. A., Perpendicular domain orientation in thin films of polystyrene - Polylactide diblock copolymers. *Macromolecules* **2005**, *38* (24), 10101-10108.
13. Baruth, A.; Rodwogin, M. D.; Shankar, A.; Erickson, M. J.; Hillmyer, M. A.; Leighton, C., Non-lift-off Block Copolymer Lithography of 25 nm Magnetic Nanodot Arrays. *ACS Appl. Mater. Interfaces* **2011**, *3* (9), 3472-3481.
14. Guo, S. W.; Rzayev, J.; Bailey, T. S.; Zalusky, A. S.; Olayo-Valles, R.; Hillmyer, M. A., Nanopore and nanobushing Arrays from ABC triblock thin films containing two etchable blocks. *Chem. Mat.* **2006**, *18* (7), 1719-1721.
15. Sinturel, C.; Vayer, M.; Morris, M.; Hillmyer, M. A., Solvent Vapor Annealing of Block Polymer Thin Films. *Macromolecules* **2013**, *46* (14), 5399-5415.
16. Han, W.; Byun, M.; Zhao, L.; Rzayev, J.; Lin, Z. Q., Controlled evaporative self-assembly of hierarchically structured bottlebrush block copolymer with nanochannels. *J. Mater. Chem.* **2011**, *21* (37), 14248-14253.
17. Han-Hao Cheng, I. K., Anguang Yu, Yami Chuang, Idriss Blakey, Kevin S. Jack, and Andrew K. Whittaker In *EUVL compatible, LER solutions using functional block copolymers*, Alternative Lithographic Technologies IV, San Jose, California, USA, 832310, Ed. SPIE: San Jose, California, USA, 2012.
18. (a) Keen, I.; Yu, A. G.; Cheng, H. H.; Jack, K. S.; Nicholson, T. M.; Whittaker, A. K.; Blakey, I., Control of the Orientation of Symmetric Poly(styrene)-block-poly(D,L-lactide) Block Copolymers Using Statistical Copolymers of Dissimilar Composition. *Langmuir* **2012**, *28* (45), 15876-15888; (b) Lo, K.-H.; Chen, M.-C.; Ho, R.-M.; Sung, H.-W., Pore-Filling Nanoporous Templates from Degradable Block Copolymers for Nanoscale Drug Delivery. *Acs Nano* **2009**, *3* (9), 2660-2666.
19. Chen, D. J.; Gong, Y. M.; He, T. B.; Zhang, F. J., Effect of crystallization on the lamellar orientation in thin films of symmetric poly(styrene)-b-poly(L-lactide) diblock copolymer. *Macromolecules* **2006**, *39* (12), 4101-4107.
20. Welander, A. M.; Kang, H. M.; Stuen, K. O.; Solak, H. H.; Muller, M.; de Pablo, J. J.; Nealey, P. F., Rapid directed assembly of block copolymer films at elevated temperatures. *Macromolecules* **2008**, *41* (8), 2759-2761.
21. Kim, S. O.; Solak, H. H.; Stoykovich, M. P.; Ferrier, N. J.; de Pablo, J. J.; Nealey, P. F., Epitaxial self-assembly of block copolymers on lithographically defined nanopatterned substrates. *Nature* **2003**, *424* (6947), 411-414.
22. Mokarian-Tabari, P.; Collins, T. W.; Holmes, J. D.; Morris, M. A., Brushless and controlled microphase separation of lamellar polystyrene-b-polyethylene oxide thin films for block copolymer nanolithography. *Journal of Polymer Science Part B-Polymer Physics* **2012**, *50* (13), 904-909.
23. Rice, R. H.; Mokarian-Tabari, P.; King, W. P.; Szoszkiewicz, R., Local Thermomechanical Analysis of a Microphase-Separated Thin Lamellar PS-b-PEO Film. *Langmuir* **2012**, *28* (37), 13503-13511.
24. Ivan Wichterle, J. L., *Antoine Vapor Pressure Constants of Pure Compounds*. 1971.
25. Ho, R. M.; Tseng, W. H.; Fan, H. W.; Chiang, Y. W.; Lin, C. C.; Ko, B. T.; Huang, B. H., Solvent-induced microdomain orientation in polystyrene-b-poly (L-lactide) diblock copolymer thin films for nanopatterning. *Polymer* **2005**, *46* (22), 9362-9377.
26. Ringardlefebvre, C.; Baszkin, A., Behavior of Poly(D,L-lactic acid) Monolayers at the Air-water-interface- Effect of Spreading Solvents. *Langmuir* **1994**, *10* (7), 2376-2381.

27. Zalusky, A. S.; Olayo-Valles, R.; Wolf, J. H.; Hillmyer, M. A., Ordered nanoporous polymers from polystyrene-poly(lactide) block copolymers. *Journal of the American Chemical Society* **2002**, *124* (43), 12761-12773.
28. Matsen, M. W.; Bates, F. S., Unifying weak- and strong-segregation block copolymer theories. *Macromolecules* **1996**, *29* (4), 1091-1098.
29. Pauling, L., *The Nature of the Chemical Bond*. 3 ed.; 1960.
30. Galema, S. A., Microwave chemistry. *Chem. Soc. Rev.* **1997**, *26* (3), 233-238.
31. Gabriel, C.; Gabriel, S.; Grant, E. H.; Halstead, B. S. J.; Mingos, D. M. P., Dielectric parameters relevant to microwave dielectric heating. *Chem. Soc. Rev.* **1998**, *27* (3), 213-223.
32. Mingos, D. M. P.; Baghurst, D. R., Applications of Microwave Dielectric Heating Effects to Synthetic Problems in Chemistry. *Chem. Soc. Rev.* **1991**, *20* (1), 1-47.
33. (a) Hung, C. G., JR The Resistivity and Hall Effect of Germanium at Low Temperatures. *PHYSICAL REVIEW* **1950**, *79* (4), 726-727; (b) Hung, C. G., JR Resistivity and Hall effect of Germanium at Low Temperatures. *Physical Review* **1954**, *96* (5), 1226-1236.
34. Tanaka, S.; Fan, H. Y., Impurity Conduction in P-Type Silicon at Microwave Frequencies. *PHYSICAL REVIEW* **1963**, *132* (4), 1516.
35. Tanaka, S.; Hanamura, E.; Kobayashi, M.; Uchinoku, K., Microwave Absorption in Silicon at Low Temperatures *Physical Review a-General Physics* **1964**, *134* (1A), A256-&.
36. Cummins, C.; Mokarian-Tabari, P.; Holmes, J. D.; Morris, M. A., Selective Etching of Poly(lactic Acid) in Poly(styrene)-block-poly(D,L)lactide Diblock Copolymer for Nanoscale Patterning. *J. Appl. Polym. Sci.* **2014**, *Fully accepted on 8th April*.
37. Gokan, H.; Esho, S.; Ohnishi, Y., Dry Etch Resistance of Organic Materials. *Journal of the Electrochemical Society* **1983**, *130* (1), 143-146.
38. Haubruge, H. G.; Jonas, A. M.; Legras, R., Staining of poly(ethylene terephthalate) by ruthenium tetroxide. *Polymer* **2003**, *44* (11), 3229-3234.